

Single-cell exploration of active phosphate-solubilizing bacteria across diverse soil matrices for sustainable phosphorus management

Received: 5 February 2024

Accepted: 10 July 2024

Published online: 05 August 2024

 Check for updates

Hong-Zhe Li^{1,2}, Jingjing Peng³, Kai Yang^{1,2}, Yiyue Zhang^{1,2}, Qing-Lin Chen¹, Yong-Guan Zhu⁴✉ & Li Cui^{1,2}✉

Phosphate-solubilizing bacteria (PSB) are crucial for enhancing phosphorus bioavailability and regulating phosphorus transformation processes. However, the in situ phosphorus-solubilizing activity and the link between phenotypes and genotypes for PSB remain unidentified. Here we employed single-cell Raman spectroscopy combined with heavy water to discern and quantify soil active PSB. Our results reveal that PSB abundance and in situ activity differed significantly between soil types and fertilization treatments. Inorganic fertilizer input was the key driver for active PSB distribution. Targeted single-cell sorting and metagenomic sequencing of active PSB uncovered several low-abundance genera that are easily overlooked within bulk soil microbiota. We elucidate the underlying functional genes and metabolic pathway, and the interplay between phosphorus and carbon cycling involved in high phosphorus solubilization activity. Our study provides a single-cell approach to exploring PSB from native environments, enabling the development of a microbial solution for the efficient agronomic use of phosphorus and mitigating the phosphorus crisis.

Phosphorus is an essential element for all living organisms. Its limited global reserves underscore the importance of efficient phosphorus management in agriculture systems^{1,2}. When phosphorus fertilizers are applied to soils, a notable portion becomes bound to soil particles due to interactions with the iron and aluminium hydroxides in acidic soils, and calcium in alkaline soils³. This creates a pool of residual phosphorus that far exceeds the requirements for crop growth but is not readily bioavailable for plant uptake. The non-renewable nature of geological phosphorus deposits, rising demand for phosphorus fertilizers and low utilization efficiency have led to the phosphorus crisis, endangering global food production. Phosphate-solubilizing

bacteria (PSB) are crucial for enhancing phosphorus bioavailability and regulating phosphorus transformation processes through the secretion of organic acid and phosphatase enzymes⁴. Their metabolic activity in the native soil habitat significantly impacts the solubilization efficiency of soil-fixed phosphorus. Understanding the in situ activity of PSB and their responses to different soil and fertilization types is fundamental for guiding efficient fertilizer application. Additionally, integrating this activity with specific taxa and genetic determinants provides a more comprehensive understanding of the mechanisms underlying the phosphorus solubilization process and offers insights for sustainable phosphorus management.

¹Key Lab of Urban Environment and Health, Institute of Urban Environment, Chinese Academy of Sciences, Xiamen, China. ²Fujian Key Laboratory of Watershed Ecology, Institute of Urban Environment, Chinese Academy of Sciences, Xiamen, China. ³China Agricultural University, Beijing, China.

⁴Research Center for Eco-Environmental Sciences, Chinese Academy of Sciences, Beijing, China. ✉e-mail: ygzhu@cees.ac.cn; lcui@iue.ac.cn

Bulk techniques, such as metagenomic sequencing, have been widely used to identify PSB and their functional genes⁵, providing valuable insights into the diversity and genetic capabilities of PSB^{6,7}. However, these techniques have limitations in resolving the specific cellular activities of individual micro-organisms. In addition, a major portion of microbial diversity (>40%) may arise from dead or dormant cells, and from extracellular DNA, and not all functional genes can be actively expressed. These factors constrain the effectiveness of genetic exploration in fully understanding the phosphorus solubilization capabilities of soil micro-organisms⁸.

A single-cell phenotypic approach is promising for directly elucidating microbial functions in their native habitats in a culture-independent manner. Fluorescent reporters in conjunction with fluorescence-activated cell sorting (FACS) can provide a way to monitor and quantify specific types of functional microbes in environments, such as cellulose-degrading bacteria, but are limited in the type of functions they can report^{9,10}. For example, FACS has not been reported to be able to discriminate PSB in soils. Nanoscale secondary ion mass spectrometry combined with stable isotope probing offers an approach to studying functional bacteria in environments by analysing the assimilated stable isotope at the single-cell level¹¹. However, this method is destructive and thus not compatible with downstream genetic sequencing. Single-cell Raman spectroscopy combined with heavy water (Raman-D₂O) has demonstrated its efficiency in probing the phenotypic traits of PSB and their phosphorus-releasing activities. This approach is based on the finding that PSB were greatly more active in assimilating D₂O than non-PSB in the presence of fixed phosphorus. The resulting C–D Raman band has been established as a biomarker for distinguishing PSB, and the intensity ratios can be utilized to quantify the phosphorus-solubilizing activities of both inorganic and organic PSB. This method provides a strategic advantage in discriminating PSB and evaluating their metabolic activity across diverse soil matrices, enabling a deeper exploration of the factors influencing phosphorus solubilization processes. The further integration with Raman-activated single-cell sorting and targeted metagenomic sequencing facilitates the investigation of both taxa and genomic attributes of active PSB^{12,13}, thereby advancing our understanding of the key players and underlying mechanisms involved in phosphorus cycling.

The microbial phosphate solubilization process in soil matrix is highly intricate and influenced by many factors, including soil types and fertilization inputs. These factors can impact the stable C:N:P stoichiometry required by PSB to maintain their activity and growth. Fertilizers have been found to exert a profound ecological impact on microbial-driven phosphorus cycling in various terrestrial ecosystems^{6,7,14,15}. For instance, Blanes et al. found that using inorganic fertilizers led to an increase in the abundance of genes associated with inorganic phosphorus solubilization¹⁶. Additionally, a fertilization-induced decrease in soil pH hindered the genetic capacity of micro-organisms to solubilize fixed inorganic phosphorus by altering the composition of the microbial community¹⁷. Despite these findings from genotypic surveys at the population level, it remains unclear how fertilizer application influences the abundances and in situ activity of PSB in different soils, which specific taxa drive the phosphorus solubilization function and the underlying metabolic processes. In addition, microbial-driven phosphorus solubilization is not solely related to inorganic and organic phosphorus release but also to carbon cycling associated with H⁺ and organic acid secretion¹⁸. However, our understanding of the interplay between the metabolic processes responsible for phosphorus solubilization and carbon cycling in the active PSB remains limited.

In this Article, we aimed to address these knowledge gaps by examining the impact of fertilization on active PSB communities across diverse soil types and elucidating the mechanisms underpinning phosphorus solubilization and carbon cycling. To achieve this, single-cell Raman-D₂O was used to quantify active soil PSB and assess their phenotypic responses, including abundance and in situ activity, to soil types

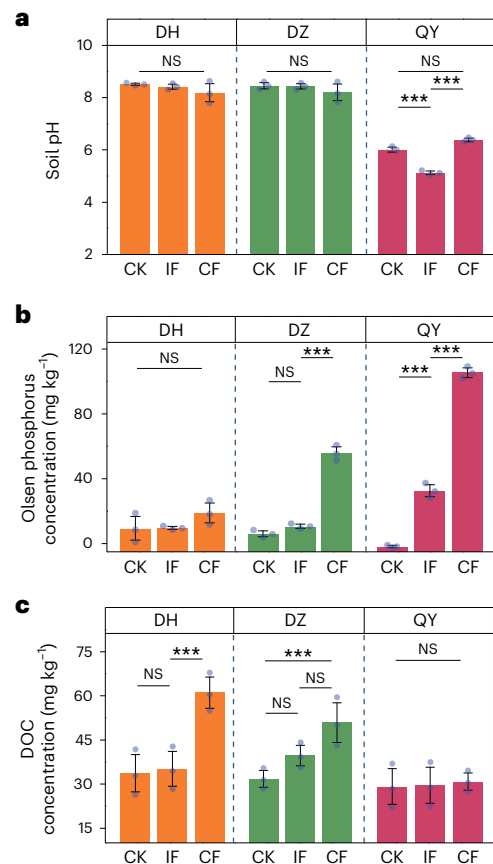


Fig. 1 | Effect of long-term fertilization on soil physicochemical properties.

a–c, Changes in soil pH (**a**), Olsen phosphorus concentration (**b**) and DOC concentration (**c**) under different fertilization regimes (CK, IF, CF) in DH, DZ and QY soils. Data are presented as mean \pm s.d. of three biological replicates. One-way ANOVA was used to test the significance: *** $P < 0.005$; NS, not significant. In **a**, QY treatments, $P = 1 \times 10^{-4}$ (CK versus IF), $P = 1 \times 10^{-5}$ (CK versus CF). In **b**, DZ treatments, $P = 1.98 \times 10^{-4}$ (IF versus CF); QY treatments, $P = 1.91 \times 10^{-4}$ (CK versus IF), $P = 1.92 \times 10^{-4}$ (IF versus CF). In **c**, DH treatments, $P = 1.08 \times 10^{-3}$ (IF versus CF); DZ treatments, $P = 1.53 \times 10^{-3}$ (CK versus CF).

and long-term fertilization practices. This phenotypic information was then leveraged to identify the key factor driving microbial phosphorus solubilization in soil. By further integration with targeted single-cell sorting and metagenomic sequencing, we elucidated the taxonomic affiliation of highly active PSB and their genomic determinants. In particular, some previously unrecognized genera exhibiting a high phosphorus solubilization capability were identified, and the underlying phosphorus and carbon cycling genes and interplay mechanisms were clarified. This work contributes to elucidating the metabolically active PSB within their natural habitat and the associated taxa and mechanisms, providing an important guide for the efficient agronomic use of phosphorus and mitigating the phosphorus crisis.

Results

Change of soil properties across different soil treatments

Understanding the in situ phosphorus solubilization ability of soil native microbes is important to utilize the legacy phosphorus abundant in soil and mitigate the phosphorus crisis. Here, three types of typical Chinese soils across northern and southern arable land receiving no fertilizer (CK), inorganic fertilizer (IF) and a combination of inorganic and organic fertilizer (CF) were studied. The soil samples from Dezhou (DZ) and Donghu (DH) were alkaline (pH > 8), and those from Qiyang (QY) were acidic (pH < 6, Fig. 1a). Application of fertilizer was found not to affect soil pH. The original Olsen phosphorus concentrations

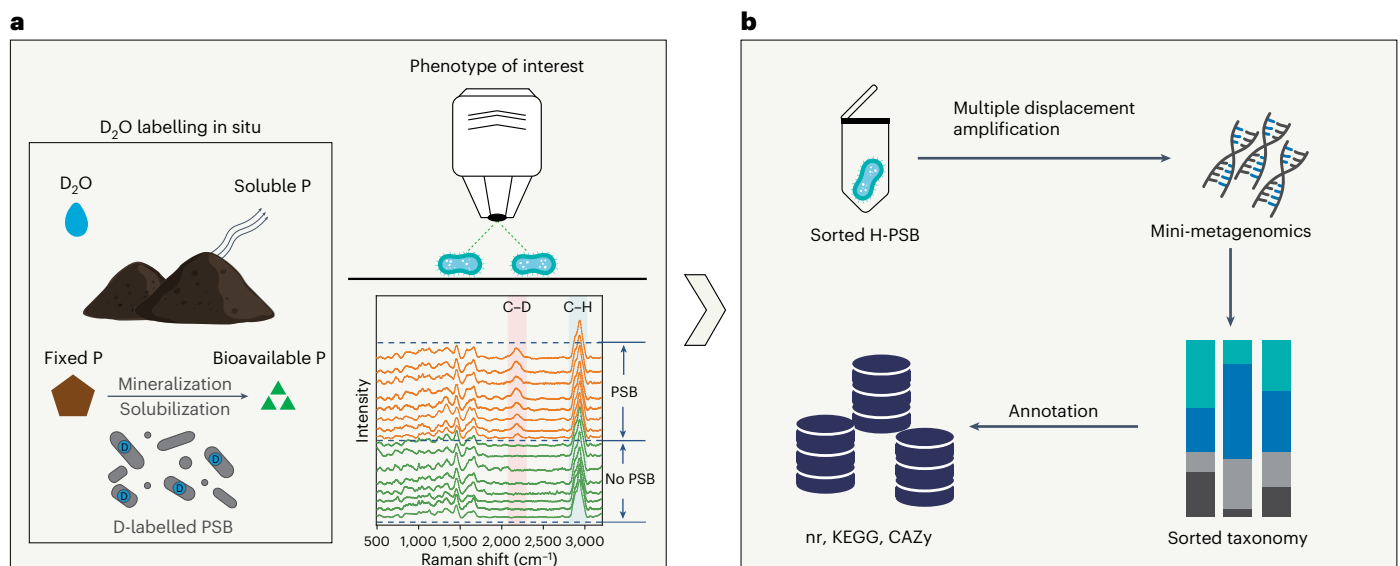


Fig. 2 | Workflow for in situ PSB identification. a, Tracking active PSB through Raman-D₂O. **b**, Analysing PSB through targeted single-cell sorting and metagenomic sequencing.

in DZ and DH soils were higher than in QY soils. The application of IF significantly increased ($P < 0.001$) Olsen phosphorus concentration in QY soils but had no effect on DZ and DH soils. In contrast, the application of CF significantly increased Olsen phosphorus concentration in DZ and QY soils ($P < 0.001$), but not in DH soils ($P > 0.05$, Fig. 1b), indicating varying phosphorus fixation and mobilization levels in different soils. In addition, application of CF significantly increased dissolved organic carbon (DOC) concentration in DH and DZ soils ($P < 0.05$), but not in QY soils ($P > 0.05$, Fig. 1c).

Quantification of in situ phosphorus solubilization ability of soil micro-organisms

Single-cell Raman-D₂O was used to detect the presence of active indigenous PSB in these soils and quantify their activities to solubilize fixed phosphorus in a culture-independent way¹⁹ (Fig. 2a). The collected soils were washed with NaHCO₃ solution to remove Olsen phosphorus until its concentration was below 2.0 mg kg⁻¹ and leave mostly fixed phosphorus in the soils (Supplementary Table 1). These nearly Olsen phosphorus-free soils were then incubated with 200 μl g⁻¹ D₂O at 27 °C for 16 h; in such soils only active PSB capable of solubilizing soil fixed phosphorus can use D₂O for their metabolism, and display a C–D Raman band (2,040–2,300 cm⁻¹) due to replacement of hydrogen by deuterium in the CHx of proteins and lipids. The C–D ratio, calculated as C–D/(C–D + C–H) (the area of each peak), represents the deuterium uptake level¹⁹. Supplementary Fig. 1a shows the C–D ratios of bacteria in the original and washed (Olsen phosphorus-free) soils. The activity (Supplementary Fig. 1a) and abundance (Supplementary Fig. 1b) of active cells (C–D ratio >8%) in the original soils were significantly higher than in the washed soils, indicating that only a fraction of soil cells can solubilize fixed phosphorus. It was also noticed that even in the original soils, the C–D ratios of soil microbes varied significantly with soil type and fertilization treatment (Supplementary Fig. 1a, $P < 0.05$), indicating that the microbial uptake level of deuterium was affected by the soil substrate pool with varying nutrient levels. To eliminate such an effect and allow comparison of PSB across different soils, normalized C–D ratios were calculated by dividing the C–D ratios from the washed soils with the average from the original soils (Fig. 3a). Active PSB were then discerned by setting a threshold at 0.5, which was determined by calculating the mean + 3 × s.d. of normalized C–D ratios of soil bacteria without incubation with D₂O (Fig. 3a)²⁰.

Using the above-defined threshold, the abundance of active PSB in different soils was calculated. The optimum number of soil bacteria required for single-cell Raman detection and abundance analysis was estimated, taking into consideration the trade-off between statistical accuracy and calculation time. Over 600 single-cell Raman spectra were detected from each soil sample (a total of ~5,400 spectra for all samples); from these, a total of 200 single-cell spectra were randomly selected from each treatment to calculate the percentage of PSB (Supplementary Fig. 2). With the increase in sample size, the variation of PSB percentage decreased until it reached a plateau for a sample size of 100 (red lines), indicating 100 single cells were appropriate for calculating the abundance of active PSB in a complex soil microbial community. The abundance of active PSB in nine soil samples was calculated and found to be dependent on both soil type and fertilization regime (Fig. 3b). DZ soils without fertilization treatment were found to contain the most abundant PSB, followed by QY and DH. In addition, fertilizer application, especially IF, further led to an increase in the active PSB abundance in DH and DZ soils ($P < 0.001$). However, in QY soils, a slight decrease in active PSB was observed under IF and CF treatments ($P < 0.05$, Fig. 3b). Because the ability of soil micro-organisms to mobilize fixed phosphorus is associated with both the abundance of PSB and their metabolic activities, these two parameters were multiplied to quantify the phenotypic microbial phosphorus solubilization efficiency (Fig. 3c). A similar trend of phosphorus mobilization efficiency to that of PSB abundance was observed but with a larger variation, indicating the highly varying activity of individual PSB cells in these soils. In addition, the effect of fertilization on the microbial community in three soil types was also investigated. IF treatment was found to greatly increase the abundance of some potential PSB and microbial interactions in comparison with CK and CF treatment (Fig. 3), partly consistent with the Raman detection. These results indicate that tailored fertilization of soils can promote microbial mobilization of soil fixed phosphorus.

To further investigate the potential factors affecting the microbial phosphorus solubilization function in different soils, the correlation of the phenotypic PSB indexes with Olsen phosphorus and DOC in soils was analysed (Supplementary Figs. 3 and 4). The percentage of PSB was found to be positively associated with low concentrations of soil Olsen phosphorus (10–35 mg kg⁻¹, CK and IF treatments) in DZ and DH soils (Supplementary Fig. 3a) but negatively correlated with

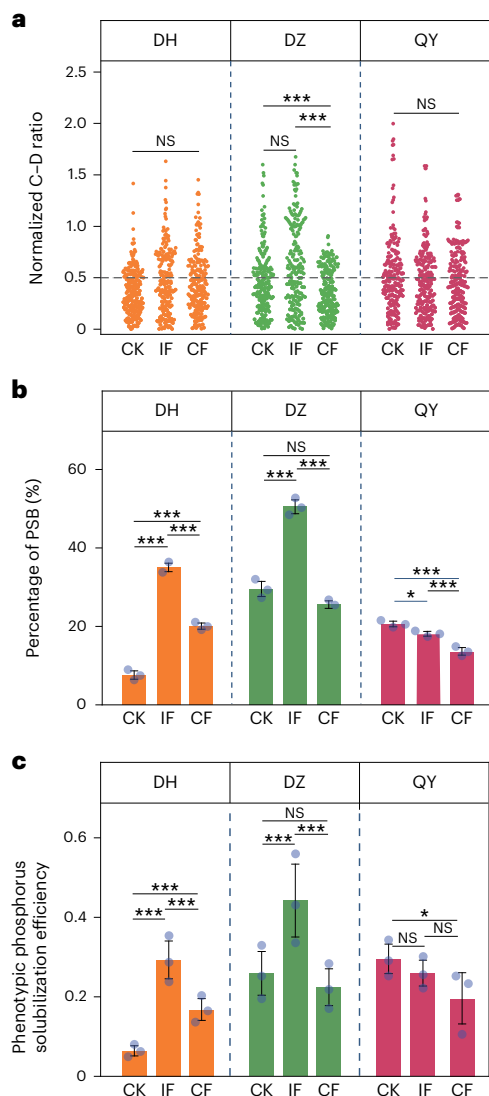


Fig. 3 | Evaluation of phenotypic microbial phosphorus solubilization of soils. **a–c**, The normalized C–D ratios (**a**), PSB percentage (**b**) and phenotypic phosphorus solubilization efficiency (**c**) in DZ, DH and QY soils. The grey dashed line at 0.5 represents the threshold for distinguishing PSB and non-PSB; this is determined as the mean + 3 × s.d. of the cell without D₂O addition (deuterium free). In **a**, $n = 200$ single-cell Raman spectra. In **b,c**, data are presented as mean ± s.d. of three biological replicates. One-way ANOVA was used to test the significance: * $P < 0.05$, *** $P < 0.005$. In **a**, DZ treatments, $P = 3.00 \times 10^{-4}$ (CK versus CF), 1.00×10^{-5} (IF versus CF). In **b**, DH treatments, $P = 3.29 \times 10^{-13}$ (CK versus IF), $P = 3.07 \times 10^{-13}$ (IF versus CF), $P = 7.33 \times 10^{-12}$ (CK versus CF); DZ treatments, $P = 2.87 \times 10^{-11}$ (CK versus IF), $P = 6.12 \times 10^{-12}$ (IF versus CF); QY treatments, $P = 4.23 \times 10^{-2}$ (CK versus IF), $P = 2.90 \times 10^{-3}$ (IF versus CF), $P = 3.00 \times 10^{-4}$ (CK versus CF). In **c**, DH treatments, $P = 1.00 \times 10^{-3}$ (CK versus IF), $P = 2.01 \times 10^{-3}$ (IF versus CF), $P = 4.27 \times 10^{-3}$ (CK versus CF); DZ treatments, $P = 7.70 \times 10^{-4}$ (CK versus IF), $P = 4.05 \times 10^{-3}$ (IF versus CF); QY treatments, $P = 4.97 \times 10^{-2}$ (CK versus IF).

high Olsen phosphorus concentrations (35–70 mg kg⁻¹, CF treatment) in these soils (Supplementary Fig. 3b). However, in QY soils, a negative correlation between Olsen phosphorus and PSB abundance was observed for both low and high concentrations of Olsen phosphorus (Supplementary Fig. 3c). Furthermore, phosphorus solubilization efficiency was associated with Olsen phosphorus in DZ and DH soils but not in QY soils (Supplementary Fig. 3g–i). The different results obtained for alkaline (DH and DZ) and acidic (QY) soils indicated that pH was an important factor affecting microbial phosphorus solubilization, and the influence of Olsen phosphorus on phenotypic phosphorus

solubilization function was dependent on both soil type and fertilization regime. Significant negative relationships were observed between the abundance of active PSB and DOC in QY soils and in both DH and DZ soils treated with IF and CF ($P < 0.05$; Supplementary Fig. 4b,c). In contrast, PSB activity was positively correlated with DOC only in DH and DZ soils with CK and IF treatment (Supplementary Fig. 4d). In most other cases, no significant correlation was observed ($P > 0.05$; Supplementary Fig. 4a,d–f,g–i).

Targeted sorting and identification of highly active indigenous PSB in soils

Non-destructive Raman detection enables single-cell sorting and targeted metagenomic sequencing of cells of interest, providing a way to link the phosphorus negative solubilization function to the specific taxa and the underlying mechanisms (Fig. 2b). A single-cell laser ejection method was used to sort out highly active PSB (H-PSB) with normalized C–D ratios >1.2 (top 7%). A total of 60 single H-PSB (20 single cells from each soil type) were sorted and sequenced. The dominant phyla in the sorted cells belonged to Firmicutes, Proteobacteria and Acidobacteriota (Fig. 4a). All the sorted PSB phyla (post-sorting) can be found in the bulk soil communities through 16S rRNA gene sequencing (pre-sorting), demonstrating their prevalence in the original bulk soil (Fig. 4a). Calculation of the relative abundance revealed that the sorted phylum of Firmicutes was present at a relatively low abundance in the initial DH (0.58%) and DZ (0.38%) soils, while they were remarkably enriched by 186- and 115-fold in the sorted fractions. The other two dominant phyla in the sorted fraction were also enriched (Fig. 4a), indicating that these phyla played a more important role in solubilizing fixed phosphorus in native soils. A further taxonomic identification revealed the sorted active PSB at the species level, including *Bacillus marmarensis* and *Bacillus pseudofirmus* in DH soils, *Moraxella osloensis* in DZ soil, and *Stenotrophomonas maltophilia* and *Cutibacterium acnes* in QY soil (Fig. 4b). These species have been previously reported as typical PSB or able to solubilize fixed phosphorus^{21–23}, supporting the result of Raman identification of phenotypic PSB. It is noteworthy that *Bacillus* and *Propionibacterium* sorted from DZ and QY soils, respectively, belonged to an unculturable genus, suggesting the existence of these efficient PSB is worth further exploration.

Genetic basis and metabolic pathways of phosphorus and carbon cycling interplay

The sorted fractions were further investigated to understand the genetic basis underlying the phosphorus solubilization function and the associated metabolism pathways. In DZ-sorted metagenome, one typical gene encoding inorganic phosphorus solubilization (*ppa*, Supplementary Fig. 5) and five genes encoding organic phosphorus acquisition, including glucose 1-dehydrogenase (*pqq*), lysophospholipase (*hch*), phospholipase A2 (*hsa*), phospholipase C (*ppp*) and glycerophosphodiester phosphodiesterase (*gly*), were found (Supplementary Fig. 6), suggesting that H-PSB in DZ soils possessed the genetic capability to recycle phosphorus from soil organic matter, especially from phospholipid and glycerophospholipid. Due to the incomplete bacterial genome from the sorted PSB and the limited number of phosphorus-cycling-related genes, we elected to search seven genomes from the NCBI database that are phylogenetically congruent with our sorted bacterial samples, which facilitated the prediction of genes involved in phosphorus cycling. These genomes were annotated against the Kyoto Encyclopedia of Genes and Genomes (KEGG) database, and a total of 24 genes associated with phosphorus metabolism were identified, including genes related to phosphorus solubilization, mineralization, regulatory functions and transporters (Fig. 5a). This finding suggests that these bacteria possess complete genetic pathways involved in the unlocking of fixed phosphorus. Our analysis revealed that *C. acnes* and *M. osloensis* had the potential to

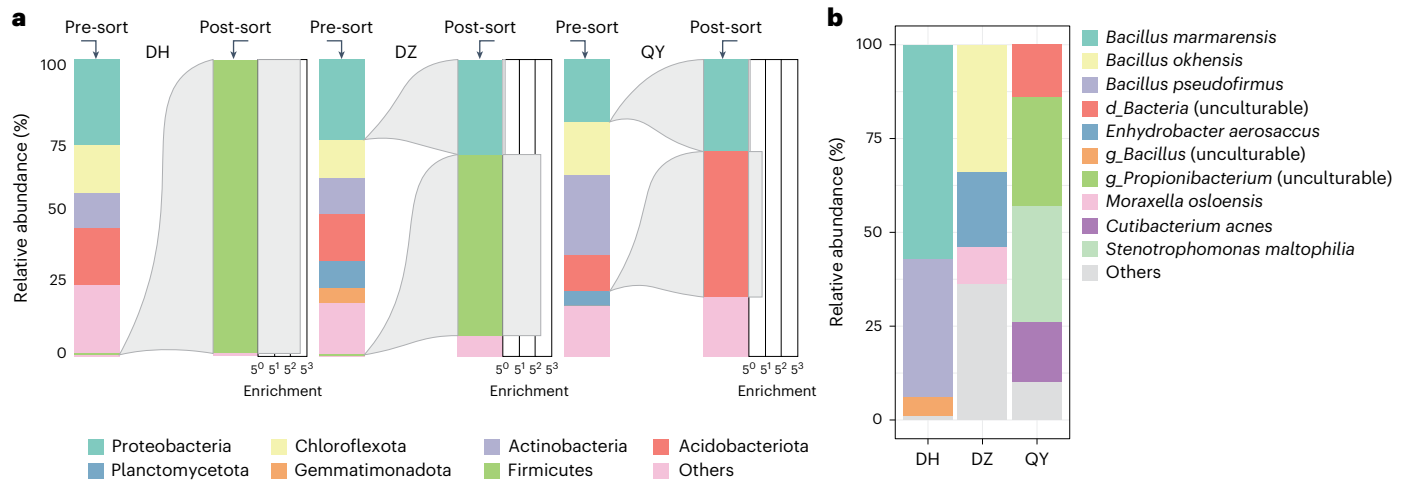


Fig. 4 | Bacterial composition of the sorted H-PSB. **a**, Sorting enrichment of H-PSB recovered from bulk soils. Relative abundance of bulk soil bacterial communities (pre-sorting) and Raman-sorted H-PSB (post-sorting) at phylum level. OTUs of bulk soil micro-organisms that match to an H-PSB that were

enriched during the sorting are marked with a grey alluvium indicating taxonomy (phylum) that links the pre- and post-sorting relative abundances. **b**, Relative abundance of the Raman-sorted H-PSB at the species level from DH, DZ and QY soils.

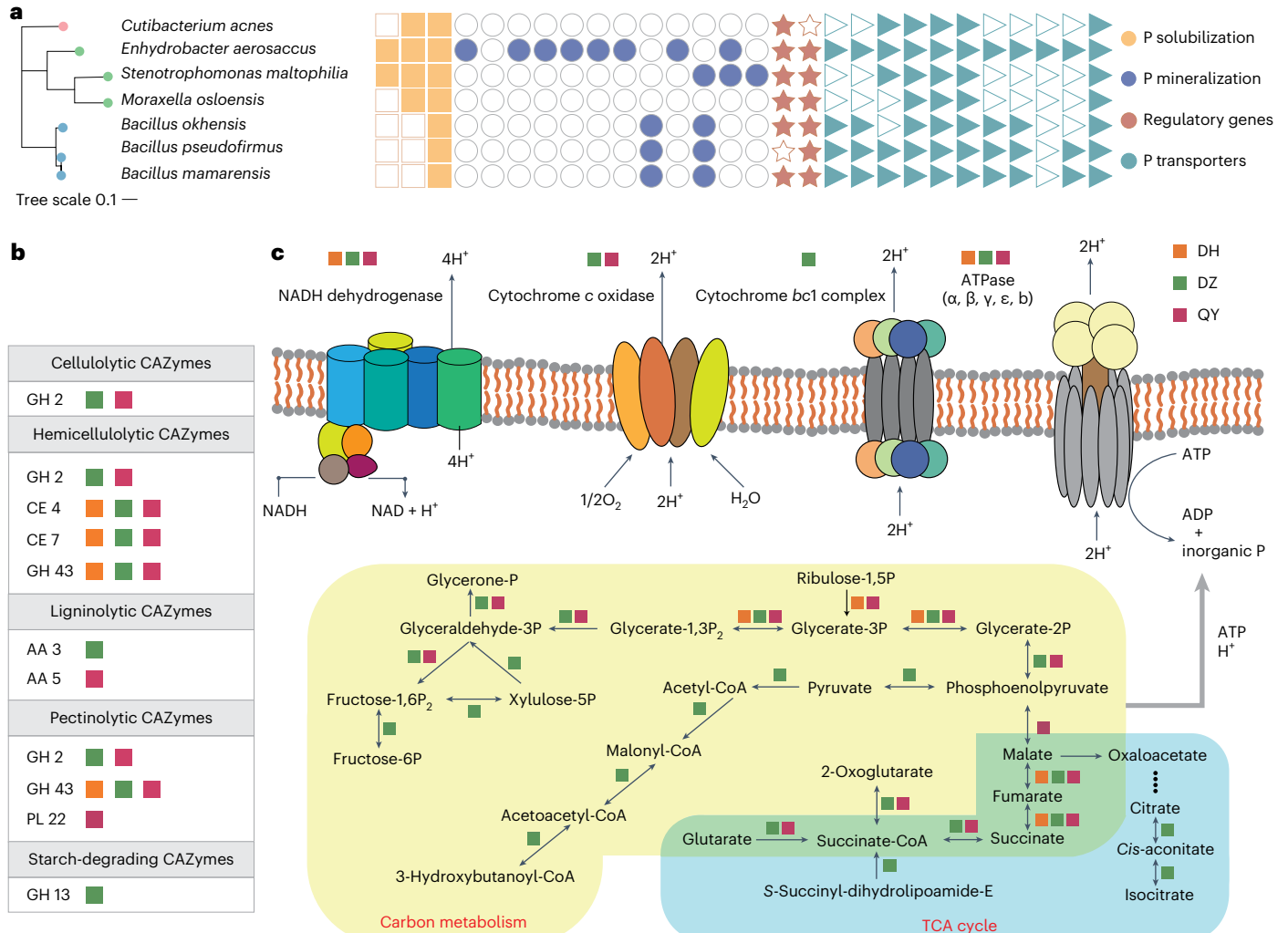


Fig. 5 | Genetic information of sorted H-PSB. **a**, Phylogenetic tree displaying the nearest neighbours of seven sorted H-PSB based on BLAST searches against the NCBI database. The heatmap shows the phosphorus-cycling-relevant functional genes in these PSB based on whole-genomic data. **b**, The detected CAZyme

groups involved in the degradation of cellulose, hemicellulose, lignin, starch and pectin. **c**, An outline of carbon metabolism and the tricarboxylic acid cycle. The coloured squares represent the presence of functional genes or enzymes.

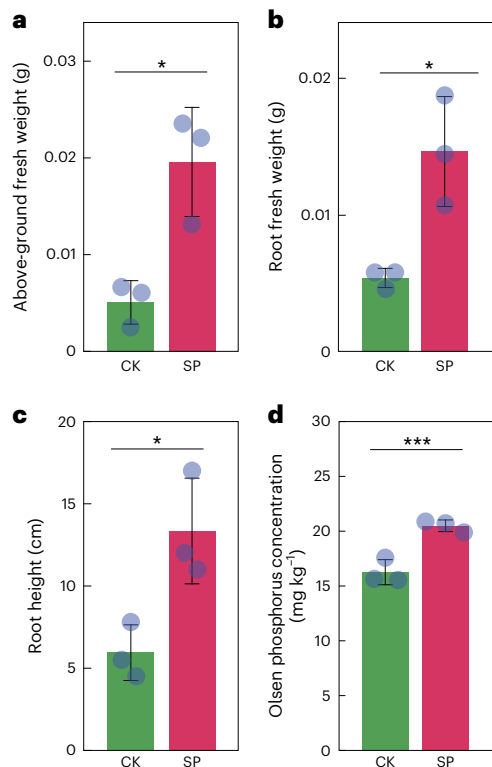


Fig. 6 | Effect of PSB addition on wheat growth and soil physicochemical properties. **a–c**, The above-ground fresh weight (**a**), root fresh weight (**b**) and plant height (**c**) were measured to illustrate the effect of PSB addition on wheat growth. **d**, Soil Olsen phosphorus concentrations were detected to examine the effects of PSB addition on releasing soil fixed phosphorus. The pot experiments included two treatments without (CK) and with addition of three sorted PSB (SP). Three biological replicates were used for each treatment. Data are presented as mean \pm s.d. A two-sided unpaired *t*-test was used for statistical significance testing: * $P < 0.05$, *** $P < 0.005$, $P = 0.0144$, $P = 0.0172$, $P = 0.0243$, $P = 0.0001$ in **a–d**, respectively.

dissolve fixed inorganic phosphorus, while *Enhydrobacter aerosaccus*, *S. maltophilia*, *Bacillus okhensis*, *B. pseudofirmus* and *B. marmarensis* possessed the capacity to release both fixed organic and inorganic phosphorus.

In addition to the phosphorus solubilization genes, carbon catabolism was also reported to participate in the inorganic phosphorus solubilization process. For instance, the anaerobic metabolism of glucose is followed by the synthesis of small molecule organic acids, which can be involved in the solubilization of fixed inorganic phosphorus²⁴. Here, a total of 22 functional genes involved in catabolism were identified in the sorted active PSB cells (Supplementary Fig. 5). Among them, the sorted cells contained genes related to pyruvate and purine metabolism, such as *pyk*, *adk*, *guaA*, *pps*, *purK*, *purE* and *guaA*. Meanwhile, the DZ sorted cells contained genes participating in pentose phosphate (*prsA*, *gntI*), oxidative phosphorylation (*ppa*), purine (*adk*, *guaB*, *purH*, *ndk*, *spoT*, *purA*, *purD*, *purT*, *nrdD*), pyruvate (*pyk*, *pps*) and pyrimidine (*thyA*, *ndk*, *dcd*, *pyrF*) catabolic pathways. All the sorted H-PSB communities contained genes encoding enzymes involved in the degradation of carbon substrates (Fig. 5b). For example, genes encoding hemicellulose and pectin degradation were detected in all sorted H-PSB cells, genes encoding cellulolytic and ligninolytic enzymes were found in DH and DZ sorted cells, and genes encoding starch-degrading enzymes were found in the DZ sorted H-PSB community.

To gain a deeper understanding of the relationship between phosphorus solubilization and carbohydrate metabolism, it is important to recognize the core metabolism that contributes to microbial

phosphorus solubilization. By annotating metagenomes of the sorted PSB against the KEGG database, the core metabolic pathways involved in carbon metabolism and the tricarboxylic acid cycle in the sorted H-PSB cells from the DZ, DH and QY soils are summarized in Fig. 5c. The carbohydrates serving as energy sources can be directly oxidized to glucose and ketones, which can then be further oxidized to produce ATP and proton^{25,26}, thereby contributing to dissolution of inorganic fixed phosphorus. In addition, enzymes, such as NADH dehydrogenase, cytochrome *c* oxidase, cytochrome *bc1* complex and ATPase, also play a critical role in generating and transferring H^+ out of cells, accelerating inorganic phosphorus solubilization²⁷.

H-PSB-promoted wheat growth and soil phosphorus solubilization

Based on the genetic profiles of sorted H-PSB (SP), strains of *M. osloensis*, *B. okhensis* and *E. aerosaccus* were selected to construct a simple synthetic community to investigate their effects on wheat growth. It is important to note that our selection of bacterial strains was contingent upon the availability of pure cultures or closely related organisms²⁸. In pot experiments, SP inoculation significantly increased above-ground fresh weight, root fresh weight and height by 285.2%, 171.8% and 125.4%, respectively (Fig. 6a–c, $P < 0.05$). Additionally, incubation with SP significantly increased the Olsen phosphorus concentration by 25.9% (Fig. 6d, $P < 0.005$).

Discussion

Application of the single-cell method in the microbial solubilization of soil phosphorus

Solubilization of the large amount of soil fixed legacy phosphorus by PSB is an effective strategy for sustainable use of phosphorus; however, identifying and quantifying metabolically active PSB inhabiting different soils, and elucidating the underlying genetic functions, are still big challenges. Single-cell Raman-D₂O has been previously demonstrated to be able to detect PSB in one type of soil, but there is a lack of standard methods for quantifying the abundance and activity of PSB in different soil types. Here, by standardizing a discrimination threshold based on the normalized activity of bacteria in Olsen phosphorus-free soils against that in original soils, single-cell Raman-D₂O was proposed to identify and quantify active indigenous PSB across different soils. This approach provides valuable insights into the in situ activity of PSB and their responses to soil types and fertilization. Further targeted single-cell sorting and metagenome sequencing of highly active PSB in soils provided a direct link between the phenotype and genotype responsible for microbial phosphorus solubilization. Specifically, it revealed key taxa, including some unculturable PSB genera with low abundances in soil microbiota, and uncovered a complex interplay between phosphorus and carbon cycling genes. This study advances our understanding of soil active PSB within complex soil communities and offers a promising microbial approach to mobilizing soil legacy phosphorus.

Compared to previous genome-centric sequencing that can only assess the potential function for phosphorus solubilization by quantifying the abundance of phosphorus functional genes (for example, *gcd*, *phod*, *pstA*)^{6,7,29–31}, this work provides a direct in situ phenotypic evaluation of microbial phosphorus solubilization function. It also provides a direct identification of the key taxa and genotypes involved in the phosphorus cycle compared to previous correlation analyses between PSB genotypes and phenotypes³². In addition, compared to bulk methods such as metagenomic sequencing and DNA stable isotope probing techniques, which struggle to resolve bacteria at low abundances, single-cell Raman sorting demonstrated its ability to meet this challenge⁹. These findings illustrate the importance of applying function-driven single-cell approaches to identify key functional micro-organisms in the soils that may be overlooked by bulk genome-based approaches.

Responses of phosphorus solubilization to soil and fertilization

Raman phenotypic characterization revealed that the abundance and phosphorus solubilization efficiency of PSB varied in three soils with three long-term fertilization treatments. In particular, PSB abundances were increased in DZ and DH soils (pH > 8) under IF treatments but decreased in acidic QY soils (pH < 6). Factors including pH, Olsen phosphorus level and DOC were revealed to influence the microbial phosphorus solubilization in different soils.

The decreased abundance of PSB in IF-treated QY soil could be due to the exacerbated soil acidification after long-term addition of chemical fertilizer. This is consistent with previous reports that found a remarkable reduction in the relative abundance of phosphorus-solubilization-related genes with decreasing pH⁷. In QY soils, low pH has been assumed to be the most common limiting factor for bacterial growth. Additionally, the extra nutrient input from fertilization could activate the originally dormant micro-organisms in QY soils (Supplementary Fig. 1), resulting in a decrease in the relative abundance of PSB (Fig. 3b).

Olsen phosphorus was revealed to have different effects on PSB abundance depending on fertilization regime. The presence of Olsen phosphorus was positively correlated with the abundance of PSB in DZ and DH soils with CK and IF treatments, reinforcing the previous view that phosphorus bioavailability regulates the biogeochemical cycle of element³³. Examination of trait-based microbial strategies when no organic matter is input indicates that microbes are driven to capture more resources for their own catabolism. For example, more micro-organisms are selected to produce extracellular enzymes to break down complex resources with increasing organic acid secretion^{34,35}, which enhances phosphorus solubilization. In contrast, negative correlations between PSB abundance and soil Olsen phosphorus were found in DZ and DH soils after organic fertilization. The absence of resource limitation favours a high-yield strategy by soil microbes³⁶. This strategy allows microbes to maximize resource uptake by allocating the added Olsen phosphorus to invest in associated assimilatory pathways, such as the synthesis of amino acids, nucleotides and fatty acids, rather than resource acquisition in which microbes are selected for catabolism processes³⁵. In addition, we found that soil bacterial community associations were more tightly linked in IF treatment, indicating cooperative and synergistic interactions among community members (Supplementary Fig. 7). These complementary activities within the community can improve overall phosphorus solubilization efficiency. Previous studies using metagenomic sequencing have also demonstrated that soil Olsen phosphorus is a main factor determining microbial phosphorus solubilization³⁷. However, the PSB activity in the three soils remains affected by Olsen phosphorus concentrations (Supplementary Fig. 3d–f). This suggests that PSB may be utilizing alternative sources of phosphorus (for example, organic compounds) or are not limited by the available phosphorus concentrations. In addition, bacteria have developed mechanisms to maintain their metabolic activity even under low-phosphorus conditions by enhancing their capability to secrete organic acids and enzymes³⁸.

Soil DOC has previously been regarded as another main factor determining microbial phosphorus solubilization according to the genotype of micro-organisms³⁹. In this study, a negative correlation between PSB abundance and DOC levels was observed in the IF- and CF-treated soils (Supplementary Fig. 4b,c), indicating that high carbon input could decrease the abundance of active PSB. One possible explanation is that elevated soil DOC may stimulate the growth of micro-organisms engaging in resource competition with PSB. In addition, in most cases except DH and DZ with CK and IF treatment (Supplementary Fig. 4d), no significant relationship was found between soil DOC and either PSB activity or phosphorus solubilization efficiency ($P > 0.05$; Supplementary Fig. 4e–i). These findings suggest that the

application of additional organic fertilizer does not necessarily enhance microbial phosphorus solubilization functions in these contexts.

The above findings about the impact of soil parameters on PSB abundance and efficiency provide tailored guides to the needs of different soils. For example, in acidic soils, lime application could be a beneficial management strategy to optimize microbial phosphorus solubilization function. In addition, organic fertilizer is not necessary and should be controlled in soils when considering the phosphorus solubilization capabilities of soil microbiome. Further testing in diverse agricultural settings is necessary to apply these findings.

Active PSB in native soils and phosphorus mobilization strategy

The non-destructive Raman approach enables downstream single-cell sorting and targeted metagenomic sequencing of H-PSB in soils. The identified H-PSB taxa included *B. marmarensis*, *B. pseudofirmus*, *M. osloensis*, *S. maltophilia* and *C. acnes* spanning three phyla: Firmicutes, Acidobacteria and Proteobacteria (Fig. 4). In addition, although the majority of the sorted bacteria have been previously reported as inorganic PSB^{21–23}, this appears to be the first time that their in situ phosphorus solubilization activity in soils has been demonstrated. This study also identified three H-PSB affiliated with uncultured bacteria, that is, *g. Bacillus*, *g. Propionibacterium* and *D. Bacteria*. Here, *g* represents genus and *D* represents domain. These PSB represent important beneficial microbial resources that are worth further exploration. Additionally, the identified H-PSB were found at low abundance in bulk soil communities; low-abundance species are increasingly being recognized as important drivers of biogeochemical cycling in terrestrial ecosystems⁴⁰.

The metagenome of the sorted PSB also sheds light on the genetic basis and functional traits in relation to phosphorus and carbon metabolism. Typical genes encoding inorganic phosphorus solubilization and organic phosphorus mobilization enzymes were detected (Supplementary Figs. 5 and 6), supporting their role in mobilizing both recalcitrant inorganic and organic phosphorus. In addition, we found several carbon-cycling-related genes that encode enzymes associated with the degradation of cellulose, hemicellulose, lignin, starch and pectin, indicating that the sorted PSB can produce protons for solubilizing recalcitrant forms of phosphorus through hydrocarbon degradation, such as organic carbon compound oxidation. The protons produced as the by-products of hydrocarbon metabolism can be transferred to the extracellular space through electron transfer mediated by cytochrome *bcl* and cytochrome *c* oxidase^{41,42}. This revealed the role of carbon-cycling processes in phosphorus solubilization that has rarely been analysed in previous studies. Among the three metagenomes analysed, the genome of sorted PSB from the DZ soil contained genes encoding the catabolism of a broad spectrum of carbon sources (Fig. 5b and Supplementary Fig. 5), suggesting they have great potential to exploit nutrient sources. Microbes with a broader catabolic capacity may, therefore, become strong candidates for long-term survival and phosphorus solubilization activity in the soil. This is attributed to the fact that microbial communities exhibiting a strong capacity for resource acquisition tend to be selected, leading to enhanced colonization ability even in challenging soil conditions, as proposed by the optimal foraging theory⁴³. This finding suggests that DZ-PSB holds potential for the development of advanced biofertilizers.

Overall, the above phenotypic and genotypic findings about active PSB in soils offer practical implications for mobilizing soil legacy phosphorus to improve phosphorus availability through two sustainable strategies. The first strategy is to stimulate native soil PSB to actively release fixed phosphorus through tailored agricultural management. The deciphered responses of PSB abundance and activity to different soil types and fertilization treatments together with the driving factor contribute substantially to guiding this strategy. The second strategy involves selecting and inoculating a specific set of bacterial

species that are customized to the needs of different soils to improve phosphorus availability. The presented function-driven single-cell approach advanced the discovery and utilization of indigenous active PSB resources. Remarkably, the *in situ* high activity of Raman-identified PSB within the original soils suggests these bacteria are potentially more effective at colonizing and then facilitating phosphorus solubilization when reintroduced into soils. This advantage is notable compared with PSB isolated through conventional culture-based methods, which may thrive in artificial culture mediums but fail to colonize and function effectively in soil environments. We demonstrated that wheat plants inoculated with Raman-identified PSB exhibited greatly enhanced growth, confirming their effectiveness in practical applications. It should be noted that these strategies are not limited to agricultural systems to enhance crop growth, but can be also applied to other human-managed ecosystems, such as urban grasslands and remediation of degraded soil to offer a sustainable way to reduce phosphorus usage and mitigate the global phosphorus crisis.

Potentials of integrating active PSB in sustainable agriculture practices

In the future, one important research area is to culture the Raman-sorted functional microbes (for example, highly active PSB in soils) and develop synthetic microbial communities (SynComs) to fully leverage the soil and plant indigenous microbiomes for sustainable agricultural production. This can be achieved by advancing high-throughput living cell sorting systems and integrating them with high-throughput cultivation systems to improve cultivation rates⁴⁴. Moreover, directly identifying the genomic content of functional bacteria enhances our understanding of their metabolic pathways and nutrient requirements. This information is crucial for cultivation, particularly for the majority of functionally important but currently unculturable microbes. It should be noted that, in addition to PSB, this activity-based single-cell approach is in principle applicable to other soil-beneficial micro-organisms important for crop growth, such as potassium/silicon-solubilizing and drought/salt-tolerant bacteria, by applying alternative abiotic stresses. The constructed SynComs consisting of multiple microbial species with distinct functions and metabolic interactions are expected to be more competent and adaptable to specific environments. These insights can be integrated together to formulate effective strategies that leverage natural microbial processes to restore soil fertility, and enhance soil health and crop productivity. Another effort should focus on improving the throughput of single-cell Raman sorting techniques and gene amplification quality to obtain more comprehensive metagenomic insights into H-PSB.

In conclusion, we employed a function-driven single-cell Raman approach to discern, quantify, sort and sequence active PSB in native soils across a wide range of soil types and fertilization regimes. The *in situ* behaviour of PSB in solubilizing phosphorus in soils and its direct link with key PSB taxa and genes involved in phosphorus and carbon cycling responsible for phosphorus solubilization were revealed. This work advances our understanding of soil active functional PSB pools and their roles in soil ecosystems. In the future, single-cell Raman-guided cultivation combined with SynComs will help to harness the power of microbial resources for a sustainable agriculture.

Methods

Soil sample collection

In this study, nine different soil samples were collected from three long-term field experiments in Hunan (QY), Zhejiang (DH) and Shandong (DZ) provinces in China. These experiments utilized three different fertilization treatments: without fertilization, inorganic fertilizer, and a combination of organic (pig manure) and inorganic fertilizers. Additional information about the long-term fertilization of the soils can be found in Supplementary Table 2. Soil samples were collected from the top layer of soil, which was less than 15 cm deep,

and three replicates were collected for each soil type. The soils were then air-dried in the dark and sieved using a 0.6 mm sieve to remove larger particles.

Analysis of soil properties

Soil pH and bioavailable nutrients (that is, DOC, Olsen phosphorus) were detected to understand the comprehensive effects of different fertilization regimes on soil systems. The pH of the soils was determined by measuring the pH of soil suspensions at a soil/water ratio of 1:1.25 (w/v). The study used a total organic carbon analyser (TOC-LCPH, Shimadzu) to detect soil DOC at a soil/water ratio of 1:1.5 (w/v). Soil Olsen phosphorus was measured using the molybdenum-blue colorimetric method, which involved extracting the nutrient using a NaHCO₃ solution⁴⁵.

Active PSB extraction

To prepare the soil for analysis without bioavailable phosphorus, we added 1 g of soil to 30 ml of 0.5 mol l⁻¹ NaHCO₃ solution, which was then incubated at 25 °C and 180 r.p.m. for 6 h. After incubation, the solution was centrifuged at 6,000g for 3 min to remove the supernatant and reserve the soil micro-organisms. This washing process was repeated three to five times until the concentration of Olsen phosphorus was low in the final supernatant. The washed soils were then air-dried at room temperature. We also weighed the soils before and after drying to calculate soil moisture. To extract soil bacteria, a certain volume of D₂O was added to the soil, and the final D₂O content reached 20% of the soil moisture. Further extraction of soil bacteria was performed by Nycodenz density-gradient separation⁴⁶. Specifically, 1 g of soil sample was homogenized in 5 ml of phosphate-buffered saline solution (PBS, containing 8 g l⁻¹ NaCl, 0.2 g l⁻¹ KCl, 1.44 g l⁻¹ Na₂HPO₄ and 0.24 g l⁻¹ KH₂PO₄) amended with 25 µl of Tween 20. The slurry was vigorously vortexed for 30 min to detach soil-associated bacteria. The solution was then added to the top of 3 ml of Nycodenz solution (4 g of Nycodenz dissolved in 5 ml of sterile water) and centrifuged at 14,000g for 60 min. The bacteria-containing layer was carefully collected into a new tube, and the collected bacteria were washed twice with ultrapure water at 5,000 r.p.m. for 3 min to remove residual PBS and other reagents.

Single-cell Raman measurement and cell sorting

To perform Raman measurements, 2 µl of as-prepared soil micro-organisms were loaded onto an aluminium foil sorting chip and air-dried at room temperature. We used a LabRAM Aramis confocal Raman microscope (HORIBA Jobin-Yvon), equipped with a 300 groove per mm grating, a 100× objective (Olympus; numerical aperture, 0.09), and a 532 nm Nd:YAG laser (Laser Quantum) to acquire Raman spectra. Each cell was typically exposed for 9 s for Raman spectra acquisition. To evaluate the metabolic activity of the cell, which quantitatively evaluates the ability of microbial phosphorus solubilization, we calculated the Raman C–D ratio¹⁹. To preprocess the obtained Raman spectra, we performed baseline correction using LabSpec5 software (HORIBA Jobin-Yvon). The intensity of the Raman band was calculated from the area of the peak. The Raman C–D ratio was calculated by dividing the intensity of the C–D peak (2,040–2,300 cm⁻¹) by the sum of the C–D peak and the C–H peak (2,800–3,100 cm⁻¹).

We considered bacteria from free bioavailable phosphorus soils containing an obvious C–D band as PSB¹⁹. To obtain targeted single PSB, we used active cell laser ejection with a PRECISCS (HOOKE Instruments). We sorted PSB from three soil samples, and 20 targeted PSB of each soil sample and one control ejection without any bacteria were sorted into a receiver. We then transferred the cells to a 200 µl tube containing cell lysis buffer (QIAGEN), and lysed the sorted cells at 65 °C for 10 min. We amplified the DNA of lysed cells using multiple displacement amplification with Phi29 DNA polymerase (QIAGEN). We checked DNA quality by PCR of the 16S rRNA gene (primer: 515 F-GTGYCAGCMGCCGCGTAA, 907R-GGACTACNVGGGTWTCTAAT)²⁰. We sequenced only samples with a positive PCR result in sorted DNA

and a negative result in the control treatment using an Illumina HiSeq X-Ten sequencer (Majorbio).

Mini-metagenome sequencing and analyses

We generated 12 gigabases of sequencing data for each sample. In total, 36 gigabases of data were obtained. To ensure data quality, we eliminated clean reads with a length of less than 50 bp and an average quality score lower than 30 using Fastp. The remaining clean reads were assembled using IDBA-UD with default parameters⁴⁷. We clustered the contigs using CD-HIT with 90% identity and 90% coverage⁴⁸. The read counts of each predicted open reading frame were calculated using htseq-count v.0.6.1 with the ‘intersection strict’ parameter, and normalized by sequencing depth and open reading frame length, which were expressed as RPKM (reads per kilobase million) values^{49,50}. The contigs were queried against the NCBI nr database using DIAMOND. Metabolic pathways and carbohydrate hydrolases in each mini-metagenomics were annotated by BLASTP against the KEGG and CAZY databases, respectively^{51,52}. To analyse the phosphorus-cycling-related functional genes within the sorted H-PSB, we acquired the complete genomes of bacterial strains that fall within the sorted bacterial category from the NCBI database. Subsequently, we constructed a phylogenetic tree using FastTree v.2.1.10⁵³. To identify the phosphorus-cycling-related genes, we performed a sequence alignment against the KEGG database. This alignment was carried out using BLASTP with a stringent E-value threshold of $\leq 10^{-5}$.

Soil DNA extraction and high-throughput sequencing

We extracted soil DNA using the DNeasy PowerSoil Kit (QIAGEN) following the manufacturer’s instructions. The concentration of soil DNA was determined using a Qubit 4 Fluorometer. We sequenced the bacterial 16S rRNA gene in the V4 region using an Illumina MiSeq PE300 platform (Majorbio). To analyse the sequencing data, we used Quantitative Insights Into Microbial Ecology (QIIME v.1.9.1)⁵⁴. High-quality sequences were assigned to operational taxonomic units (OTUs) using UCLUST based on a similarity threshold of 97%. We assigned representative OTUs using the PyNAST aligner based on the SILVA database v.132⁵⁵. The raw reads of nine amplicons and three mini-metagenomics were deposited in the NCBI sequence Read Archive.

Preparation of PSB suspension and pot experiments

Three PSB strains of *M. osloensis*, *B. okhensis* and *E. aerosaccus* were purchased from BioWB. Each strain was cultured in 50 ml of LB liquid medium and incubated at 30 °C. Upon reaching an OD₆₀₀ of 0.8, the cultures were washed three times with ultrapure water to remove residual media. A mixed bacterial suspension was prepared by combining equal volumes of each bacterial culture. For the pot experiments, 10 ml of the bacterial suspension was inoculated into the root zone of each pot using a sterile syringe. Wheat seeds (Zhoumai 22) were surface-sterilized with 10% hydrogen peroxide for 15 min and vernalized at 4 °C for 48 h. Each pot contained 500 g of unfertilized soil from Dezhou, which had been washed five times with 0.5 M NaHCO₃ solution and ultrapure water to reduce Olsen phosphorus concentrations. The pots were placed in a greenhouse, and the experiment was conducted over a period of 30 days.

Statistical analyses

Shapiro–Wilk analysis was applied to test for normality. One-way analysis of variance (ANOVA) and *t*-tests performed with GraphPad Prism 5 and Excel 16.83 were used for all statistical examinations, and a *P* value < 0.05 was considered significant. Adobe Illustrator 2024 and Origin 2021 were used for data visualization.

Reporting summary

Further information on research design is available in the Nature Portfolio Reporting Summary linked to this article.

Data availability

The raw sequence data reported in this paper have been uploaded to the NCBI nr database under accession number [PRJNA1090601](https://doi.org/10.1038/s43016-024-01024-8). The relevant data are available within the Article and its Supplementary Information. Source data are provided with this paper.

References

- Karl, D. M. Phosphorus, the staff of life. *Nature* **406**, 31–33 (2000).
- Mogollón, J. M. et al. More efficient phosphorus use can avoid cropland expansion. *Nat. Food* **2**, 509–518 (2021).
- Vitousek, P. M., Porder, S., Houlton, B. Z. & Chadwick, O. A. Terrestrial phosphorus limitation: mechanisms, implications, and nitrogen–phosphorus interactions. *Ecol. Appl.* **20**, 5–15 (2010).
- Sperber, J. I. Solution of mineral phosphates by soil bacteria. *Nature* **180**, 994–995 (1957).
- Schloss, P. D. & Handelsman, J. Toward a census of bacteria in soil. *PLoS Comput. Biol.* **2**, e92 (2006).
- Wu, X. et al. Genome-resolved metagenomics reveals distinct phosphorus acquisition strategies between soil microbiomes. *Msystems* **7**, e01107–e01121 (2022).
- Dai, Z. et al. Long-term nutrient inputs shift soil microbial functional profiles of phosphorus cycling in diverse agroecosystems. *ISME J.* **14**, 757–770 (2020).
- Carini, P. et al. Relic DNA is abundant in soil and obscures estimates of soil microbial diversity. *Nat. Microbiol.* **2**, 16242 (2016).
- Doud, D. F. et al. Function-driven single-cell genomics uncovers cellulose-degrading bacteria from the rare biosphere. *ISME J.* **14**, 659–675 (2020).
- Hatzenpichler, R. et al. Visualizing in situ translational activity for identifying and sorting slow-growing archaeal–bacterial consortia. *Proc. Natl Acad. Sci. USA* **113**, E4069–E4078 (2016).
- Li, T. et al. Simultaneous analysis of microbial identity and function using NanoSIMS. *Environ. Microbiol.* **10**, 580–588 (2008).
- Lee, K. S. et al. An automated Raman-based platform for the sorting of live cells by functional properties. *Nat. Microbiol.* **4**, 1035–1048 (2019).
- Song, Y. et al. Raman-deuterium isotope probing for in-situ identification of antimicrobial resistant bacteria in Thames River. *Sci. Rep.* **7**, 16648 (2017).
- Mack, M. C., Schuur, E. A., Bret-Harte, M. S., Shaver, G. R. & Chapin, F. S. Ecosystem carbon storage in arctic tundra reduced by long-term nutrient fertilization. *Nature* **431**, 440–443 (2004).
- Oliverio, A. M. et al. The role of phosphorus limitation in shaping soil bacterial communities and their metabolic capabilities. *mBio* <https://doi.org/10.1128/mbio.01718-20> (2020).
- Blanes, M. C., Viñepla, B., Salido, M. T. & Carreira, J. A. Coupled soil-availability and tree-limitation nutritional shifts induced by N deposition: insights from N to P relationships in *Abies pinsapo* forests. *Plant Soil* **366**, 67–81 (2013).
- Rousk, J. et al. Soil bacterial and fungal communities across a pH gradient in an arable soil. *ISME J.* **4**, 1340–1351 (2010).
- Lin, X. et al. Microbial metabolic potential for carbon degradation and nutrient (nitrogen and phosphorus) acquisition in an ombrotrophic peatland. *Appl. Environ. Microbiol.* **80**, 3531–3540 (2014).
- Li, H.-Z. et al. D₂O-isotope-labeling approach to probing phosphate-solubilizing bacteria in complex soil communities by single-cell Raman spectroscopy. *Anal. Chem.* **91**, 2239–2246 (2019).
- Li, H.-Z. et al. Active antibiotic resistome in soils unraveled by single-cell isotope probing and targeted metagenomics. *Proc. Natl Acad. Sci. USA* **119**, e2201473119 (2022).

21. He, Z., Bian, W. & Zhu, J. Screening and identification of microorganisms capable of utilizing phosphate adsorbed by goethite. *Commun. Soil Sci. Plant Anal.* **33**, 647–663 (2002).
22. Keshari, S. et al. Skin *Cutibacterium acnes* mediates fermentation to suppress the calcium phosphate-induced itching: a butyric acid derivative with potential for uremic pruritus. *J. Clin. Med.* **9**, 312 (2020).
23. Xiao, C.-Q., Chi, R.-A., He, H. & Zhang, W.-X. Characterization of tricalcium phosphate solubilization by *Stenotrophomonas maltophilia* YC isolated from phosphate mines. *J. Cent. South Univ. Technol.* **16**, 581–587 (2009).
24. Alori, E. T., Glick, B. R. & Babalola, O. O. Microbial phosphorus solubilization and its potential for use in sustainable agriculture. *Front. Microbiol.* **8**, 971 (2017).
25. Bender, D. A. *Amino Acid Metabolism* (John Wiley, 2012).
26. Doelle, H. W. *Bacterial Metabolism* (Academic Press, 2014).
27. Martínez, I., Zhu, J., Lin, H., Bennett, G. N. & San, K.-Y. Replacing *Escherichia coli* NAD-dependent glyceraldehyde 3-phosphate dehydrogenase (GAPDH) with a NADP-dependent enzyme from *Clostridium acetobutylicum* facilitates NADPH dependent pathways. *Metab. Eng.* **10**, 352–359 (2008).
28. Pereira, F. C. et al. Rational design of a microbial consortium of mucosal sugar utilizers reduces *Clostridiodes difficile* colonization. *Nat. Commun.* **11**, 5104 (2020).
29. Liang, J.-L. et al. Novel phosphate-solubilizing bacteria enhance soil phosphorus cycling following ecological restoration of land degraded by mining. *ISME J.* **14**, 1600–1613 (2020).
30. Hsieh, Y.-J. & Wanner, B. L. Global regulation by the seven-component Pi signaling system. *Curr. Opin. Microbiol.* **13**, 198–203 (2010).
31. Liu, W. et al. Active phoD-harboring bacteria are enriched by long-term organic fertilization. *Soil Biol. Biochem.* **152**, 108071 (2021).
32. Li, H. et al. Single-cell Raman and functional gene analyses reveal microbial P solubilization in agriculture waste-modified soils. *mLife* **2**, 190–200 (2023).
33. Yao, Q. et al. Community proteogenomics reveals the systemic impact of phosphorus availability on microbial functions in tropical soil. *Nat. Ecol. Evol.* **2**, 499–509 (2018).
34. Allison, S. D., Wallenstein, M. D. & Bradford, M. A. Soil-carbon response to warming dependent on microbial physiology. *Nat. Geosci.* **3**, 336–340 (2010).
35. Malik, A. A. et al. Defining trait-based microbial strategies with consequences for soil carbon cycling under climate change. *ISME J.* **14**, 1–9 (2020).
36. Lipson, D. A. The complex relationship between microbial growth rate and yield and its implications for ecosystem processes. *Front. Microbiol.* **6**, 615 (2015).
37. Wu, X., Cui, Z., Peng, J., Zhang, F. & Liesack, W. Genome-resolved metagenomics identifies the particular genetic traits of phosphate-solubilizing bacteria in agricultural soil. *ISME Commun.* **2**, 17 (2022).
38. Deubel, A. & Merbach, W. in *Microorganisms in Soils: Roles in Genesis and Functions* (eds Varma, A. & Buscot, F.) 177–191 (Springer, 2005).
39. Brucker, E., Kernchen, S. & Spohn, M. Release of phosphorus and silicon from minerals by soil microorganisms depends on the availability of organic carbon. *Soil Biol. Biochem.* **143**, 107737 (2020).
40. Jousset, A. et al. Where less may be more: how the rare biosphere pulls ecosystems strings. *ISME J.* **11**, 853–862 (2017).
41. Trumppower, B. L. Cytochrome bc1 complexes of microorganisms. *Microbiol. Rev.* **54**, 101–129 (1990).
42. Wikstrom, M. K. Proton pump coupled to cytochrome c oxidase in mitochondria. *Nature* **266**, 271–273 (1977).
43. Tilman, D. *Resource Competition and Community Structure* (Princeton Univ. Press, 2020).
44. Wang, X. et al. Robust spontaneous Raman flow cytometry for single-cell metabolic phenome profiling via pDEP-DLD-RFC. *Adv. Sci.* **10**, 2207497 (2023).
45. Rodriguez, J., Self, J. & Soltanpour, P. Optimal conditions for phosphorus analysis by the ascorbic acid–molybdenum blue method. *Soil Sci. Soc. Am. J.* **58**, 866–870 (1994).
46. Eichorst, S. A. et al. Advancements in the application of NanoSIMS and Raman microspectroscopy to investigate the activity of microbial cells in soils. *FEMS Microbiol. Ecol.* **91**, fiv106 (2015).
47. Peng, Y., Leung, H. C., Yiu, S.-M. & Chin, F. Y. IDBA-UD: a de novo assembler for single-cell and metagenomic sequencing data with highly uneven depth. *Bioinformatics* **28**, 1420–1428 (2012).
48. Fu, L., Niu, B., Zhu, Z., Wu, S. & Li, W. CD-HIT: accelerated for clustering the next-generation sequencing data. *Bioinformatics* **28**, 3150–3152 (2012).
49. Anders, S., Pyl, P. T. & Huber, W. HTSeq—a Python framework to work with high-throughput sequencing data. *Bioinformatics* **31**, 166–169 (2015).
50. Mortazavi, A., Williams, B. A., McCue, K., Schaeffer, L. & Wold, B. Mapping and quantifying mammalian transcriptomes by RNA-Seq. *Nat. Methods* **5**, 621–628 (2008).
51. Kanehisa, M. & Goto, S. KEGG: Kyoto Encyclopedia of Genes and Genomes. *Nucleic Acids Res.* **28**, 27–30 (2000).
52. Lombard, V., Golaconda Ramulu, H., Drula, E., Coutinho, P. M. & Henrissat, B. The carbohydrate-active enzymes database (CAZy) in 2013. *Nucleic Acids Res.* **42**, D490–D495 (2014).
53. R Core Team R: *A Language and Environment for Statistical Computing* (R Foundation for Statistical Computing, 2013).
54. Caporaso, J. G. et al. QIIME allows analysis of high-throughput community sequencing data. *Nat. Methods* **7**, 335–336 (2010).
55. Quast, C. et al. The SILVA ribosomal RNA gene database project: improved data processing and web-based tools. *Nucleic Acids Res.* **41**, D590–D596 (2012).

Acknowledgements

This work was supported by the National Natural Science Foundation of China (grant numbers 42021005, 22241603) and the Chinese Academy of Sciences (ZDBS-LY-DQC027).

Author contributions

H.-Z.L., L.C. and Y.-G.Z. conceived the study. H.-Z.L. and K.Y. performed the experiments. H.-Z.L., J.P. and Y.Z. performed the data analysis. L.C. and Y.-G.Z. provided financial support. H.-Z.L. wrote the paper. L.C., Q.-L.C. and Y.-G.Z. reviewed and edited the paper.

Competing interests

The authors declare no competing interests.

Additional information

Supplementary information The online version contains supplementary material available at <https://doi.org/10.1038/s43016-024-01024-8>.

Correspondence and requests for materials should be addressed to Yong-Guan Zhu or Li Cui.

Peer review information *Nature Food* thanks Ying Ma, Josep Penuelas, Zhong Wei and the other, anonymous, reviewer(s) for their contribution to the peer review of this work.

Reprints and permissions information is available at www.nature.com/reprints.

Publisher's note Springer Nature remains neutral with regard to jurisdictional claims in published maps and institutional affiliations.

Springer Nature or its licensor (e.g. a society or other partner) holds exclusive rights to this article under a publishing agreement with

the author(s) or other rightsholder(s); author self-archiving of the accepted manuscript version of this article is solely governed by the terms of such publishing agreement and applicable law.

© The Author(s), under exclusive licence to Springer Nature Limited 2024

Reporting Summary

Nature Portfolio wishes to improve the reproducibility of the work that we publish. This form provides structure for consistency and transparency in reporting. For further information on Nature Portfolio policies, see our [Editorial Policies](#) and the [Editorial Policy Checklist](#).

Statistics

For all statistical analyses, confirm that the following items are present in the figure legend, table legend, main text, or Methods section.

- | n/a | Confirmed |
|-------------------------------------|------------------------------------------------------------------------------------------------------------------------------------------------------------------------------------------------------------------------------------------------------------------------------------------------|
| <input type="checkbox"/> | <input checked="" type="checkbox"/> The exact sample size (n) for each experimental group/condition, given as a discrete number and unit of measurement |
| <input type="checkbox"/> | <input checked="" type="checkbox"/> A statement on whether measurements were taken from distinct samples or whether the same sample was measured repeatedly |
| <input type="checkbox"/> | <input checked="" type="checkbox"/> The statistical test(s) used AND whether they are one- or two-sided
<i>Only common tests should be described solely by name; describe more complex techniques in the Methods section.</i> |
| <input checked="" type="checkbox"/> | <input type="checkbox"/> A description of all covariates tested |
| <input type="checkbox"/> | <input checked="" type="checkbox"/> A description of any assumptions or corrections, such as tests of normality and adjustment for multiple comparisons |
| <input type="checkbox"/> | <input checked="" type="checkbox"/> A full description of the statistical parameters including central tendency (e.g. means) or other basic estimates (e.g. regression coefficient) AND variation (e.g. standard deviation) or associated estimates of uncertainty (e.g. confidence intervals) |
| <input type="checkbox"/> | <input checked="" type="checkbox"/> For null hypothesis testing, the test statistic (e.g. F , t , r) with confidence intervals, effect sizes, degrees of freedom and P value noted
<i>Give P values as exact values whenever suitable.</i> |
| <input checked="" type="checkbox"/> | <input type="checkbox"/> For Bayesian analysis, information on the choice of priors and Markov chain Monte Carlo settings |
| <input checked="" type="checkbox"/> | <input type="checkbox"/> For hierarchical and complex designs, identification of the appropriate level for tests and full reporting of outcomes |
| <input checked="" type="checkbox"/> | <input type="checkbox"/> Estimates of effect sizes (e.g. Cohen's d , Pearson's r), indicating how they were calculated |

Our web collection on [statistics for biologists](#) contains articles on many of the points above.

Software and code

Policy information about [availability of computer code](#)

Data collection

Data analysis

For manuscripts utilizing custom algorithms or software that are central to the research but not yet described in published literature, software must be made available to editors and reviewers. We strongly encourage code deposition in a community repository (e.g. GitHub). See the Nature Portfolio [guidelines for submitting code & software](#) for further information.

Data

Policy information about [availability of data](#)

All manuscripts must include a [data availability statement](#). This statement should provide the following information, where applicable:

- Accession codes, unique identifiers, or web links for publicly available datasets
- A description of any restrictions on data availability
- For clinical datasets or third party data, please ensure that the statement adheres to our [policy](#)

The raw sequence data reported in this paper have been uploaded to NCBI nr database under the accession number PRJNA1090601. The relevant data are available within the manuscript and its Supplementary Information file.

Research involving human participants, their data, or biological material

Policy information about studies with [human participants or human data](#). See also policy information about [sex, gender \(identity/presentation\), and sexual orientation](#) and [race, ethnicity and racism](#).

Reporting on sex and gender	N/A
Reporting on race, ethnicity, or other socially relevant groupings	N/A
Population characteristics	N/A
Recruitment	N/A
Ethics oversight	N/A

Note that full information on the approval of the study protocol must also be provided in the manuscript.

Field-specific reporting

Please select the one below that is the best fit for your research. If you are not sure, read the appropriate sections before making your selection.

Life sciences Behavioural & social sciences Ecological, evolutionary & environmental sciences

For a reference copy of the document with all sections, see nature.com/documents/nr-reporting-summary-flat.pdf

Ecological, evolutionary & environmental sciences study design

All studies must disclose on these points even when the disclosure is negative.

Study description	In this study, we used single-cell Raman-D2O to discern and quantify soil active phosphate solubilizing bacteria (PSB) across various soil types and fertilization regimes. We quantified the abundance and activity of active PSB, analyzing a total of 5400 spectra from all samples. Further targeted single-cell sorting and metagenomic sequencing of active PSB uncovered several novel, low-abundance genera that are easily overlooked within bulk soil microbiota. This study provides a new single-cell approach to exploring PSB from native environments, enabling the development of microbial solutions for sustainable phosphorus utilization in agriculture.
Research sample	In this study, nine different soil samples were collected from three long-term field experiments in Hunan (QY), Zhejiang (DH), and Shandong (DZ) provinces in China. These experiments utilized three different fertilization treatments: no fertilization, inorganic fertilizer, and combined organic (pig manure) and inorganic fertilizers. These treatments represent the most prevalent practices in the studied areas. For the pot experiment, wheat samples were taken from the Zhoumai 22 variety.
Sampling strategy	For soil samples: The soil samples were collected from the top layer of soil, less than 15 cm deep, with three replicates for each soil type. The soils were then air-dried in the dark and sieved through a 0.6 mm sieve to remove larger particles. For Raman detection: A total of 200 single-cell spectra were randomly selected from each treatment to calculate the percentage of PSB. As the sample size increased, the variation in PSB percentage decreased until reaching a plateau at a sample size of 100, indicating that 100 single cells were appropriate for calculating the abundance of active PSB in a complex soil microbial community. For plant samples: The fresh weight of both root and above-ground parts was measured after sampling.
Data collection	All the data were measured and recorded by Hong-Zhe Li. The pH of the soils was determined by measuring the pH of soil suspensions at a soil/water ratio of 1:1.25 (w/v). The study used a TOC analyzer (TOC-LCPH, Shimadzu, Japan) to detect the soil DOC at a soil/water ratio of 1:1.5 (w/v). Soil Olsen-P was measured using the molybdenum-blue colorimetric method. Single-cell Raman-D2O was used to detect the activity of bacteria. We used Active Cell Laser Ejection (ACLE) with PRECI SCS (HOOKE Instruments Ltd, China) to obtain the targeted single PSB. Metagenome sequencing was used to analyze the genotypic information of PSB.
Timing and spatial scale	The soils were sampled from three long-term field experiments in Qiyang, Hunan province; Donghu, Zhejiang province; and Dezhou, Shandong province in China. The pot experiments lasted from April 4, 2024, to May 4, 2024.
Data exclusions	No data were excluded from the analyses.
Reproducibility	The findings in this paper were remarkably reproducible. For the Raman detection and plant pot experiments, we independently performed each experiment at least three times.
Randomization	The single-cell spectra were randomly selected from each soil treatment. The pot experiments were randomly assigned to different treatments.
Blinding	All soil sample processing and Raman detection were performed without signs or labels indicating the relevant treatment.

Did the study involve field work? Yes No

Reporting for specific materials, systems and methods

We require information from authors about some types of materials, experimental systems and methods used in many studies. Here, indicate whether each material, system or method listed is relevant to your study. If you are not sure if a list item applies to your research, read the appropriate section before selecting a response.

Materials & experimental systems

n/a	Involvement in the study
<input checked="" type="checkbox"/>	<input type="checkbox"/> Antibodies
<input checked="" type="checkbox"/>	<input type="checkbox"/> Eukaryotic cell lines
<input checked="" type="checkbox"/>	<input type="checkbox"/> Palaeontology and archaeology
<input checked="" type="checkbox"/>	<input type="checkbox"/> Animals and other organisms
<input checked="" type="checkbox"/>	<input type="checkbox"/> Clinical data
<input checked="" type="checkbox"/>	<input type="checkbox"/> Dual use research of concern
<input type="checkbox"/>	<input checked="" type="checkbox"/> Plants

Methods

n/a	Involvement in the study
<input checked="" type="checkbox"/>	<input type="checkbox"/> ChIP-seq
<input checked="" type="checkbox"/>	<input type="checkbox"/> Flow cytometry
<input checked="" type="checkbox"/>	<input type="checkbox"/> MRI-based neuroimaging

Dual use research of concern

Policy information about [dual use research of concern](#)

Hazards

Could the accidental, deliberate or reckless misuse of agents or technologies generated in the work, or the application of information presented in the manuscript, pose a threat to:

No	Yes
<input checked="" type="checkbox"/>	<input type="checkbox"/> Public health
<input checked="" type="checkbox"/>	<input type="checkbox"/> National security
<input checked="" type="checkbox"/>	<input type="checkbox"/> Crops and/or livestock
<input checked="" type="checkbox"/>	<input type="checkbox"/> Ecosystems
<input checked="" type="checkbox"/>	<input type="checkbox"/> Any other significant area

Experiments of concern

Does the work involve any of these experiments of concern:

No	Yes
<input checked="" type="checkbox"/>	<input type="checkbox"/> Demonstrate how to render a vaccine ineffective
<input checked="" type="checkbox"/>	<input type="checkbox"/> Confer resistance to therapeutically useful antibiotics or antiviral agents
<input checked="" type="checkbox"/>	<input type="checkbox"/> Enhance the virulence of a pathogen or render a nonpathogen virulent
<input checked="" type="checkbox"/>	<input type="checkbox"/> Increase transmissibility of a pathogen
<input checked="" type="checkbox"/>	<input type="checkbox"/> Alter the host range of a pathogen
<input checked="" type="checkbox"/>	<input type="checkbox"/> Enable evasion of diagnostic/detection modalities
<input checked="" type="checkbox"/>	<input type="checkbox"/> Enable the weaponization of a biological agent or toxin
<input checked="" type="checkbox"/>	<input type="checkbox"/> Any other potentially harmful combination of experiments and agents

Plants

Seed stocks

The wheat seeds (Zhoumai 22) were collected in the experimental field of biological interaction and ecological security in Henan University in Oct. 2023.

Novel plant genotypes

The genotypes of wheat were not considered in this study.

Authentication

N/A